MICROCOPY RESOLUTION TEST CHART
NATIONAL BUREAU OF STANDARDS-1963-A

Department of Oceanography

THE MERGING OF ISOLATED LENSES

AD-A181 561

Technical Report

DN-86-04

DTIC
S ELECTE
JUN 1 9 1987
D
D

Doron Nof

April 1986

07   4 8.003

ABSTRACT

The interaction of two isolated lens-like eddies is examined with the aid of an inviscid nonlinear model. The barotropic layer in which the lenses are embedded is infinitely deep so that there is no interaction between the eddies unless their edges touch each other. It is assumed that the latter is brought about by a mean flow which relaxes after pushing the eddies against each other and forming a "figure eight" structure.

Using arguments based on continuity and conservation of energy along the eddies edge it is shown that, once a "figure eight" shape is established, intrusions along the eddies' peripheries are generated. These intrusions resemble "arms" or "tentacles" and their structure gives the impression that one vortex is "hugging" the other. As time goes on the tentacles become longer and longer and, ultimately, the eddies are entirely converted into very long spiral-like tentacles. These spiraled tentacles are adjacent to each other so that the final result is a single vortex containing the fluid of the two parent eddies.

Because of the inherent nonlinearity and the fact that the problem is three-dimensional (x, y, t), the complete details of the above process cannot be described analytically. It is, however, possible to show analytically that the intrusions and tentacles are inevitable. For this purpose, one of the interacting eddies is conceptually replaced by a solid cylinder. Initially, the cylinder drifts toward the eddy; subsequently, it is pushed slightly into the eddy and is then held fixed. The subsequent events are examined in detail.

It is found that as the cylinder is forced into the eddy, a band of eddy water starts enveloping the cylinder in a clockwise manner. This tentacle continues to intrude along the cylinder perimeter until it

ultimately reattaches itself to the eddy, forming a "padlock" flow. Using the details of this process it is argued that, in the actual eddy-eddy interaction case, intrusions must be established and that, consequently, merging of the two eddies is inevitable.

1. Introduction

Isolated lens-like eddies are common in many parts of the ocean; they usually result from meandering currents which close upon themselves and pinch-off (see e.g., The Ring Group 1981, Lai and Richardson 1977, Cheney 1977). Their abundance in the ocean and the, almost permanent, presence of mean currents suggest that collisions of eddies are probably a fairly common occurrence. The processes associated with eddy collisions and the resulting encounters are the focus of the present study.

a) <u>Background</u>: So far, there has been only one set of observations of a direct eddy-eddy interaction (Cresswell, 1982, Cresswell and Legeckis 1986). In this case, two anticyclonic lens-like eddies have collided in the vicinity of the East Australian Current. Initially, they moved around each other but within a period of about 20 days they have completely merged (Fig. 1). These observations have generated the interest of Gill and Griffiths (1981) who, in a short communication, have pointed out that if two inviscid eddies with zero potential vorticity are forced to merge and conserve their potential vorticity during the merging, then the final vortex would have energy that is larger than the sum of the individual energies.

This conclusion can be easily demonstrated by considering the velocity and depth of a zero potential vorticity vortex (see e.g., Nof 1981a,b),

$$v_{\theta i} = -fr/2 \quad ; \quad h_i = \hat{h}_i - f^2 r/8g' \; , \qquad (1.1)$$

where v_i and h_i are the tangential velocity[1] and depth, f the Coriolis parameter, g' the "reduced gravity" [$(g\Delta\rho/\rho)$, with g the gravitational acceleration, $\Delta\rho$ the density difference between the layers and ρ the eddy density)], and $\hat{h}_i$ is the depth at the center of the vortex [i.e., $\hat{h}_i = h_i(0)$]. Here, the subscript "i" indicates that the variable in question is associated with the initial state (prior to any interaction or merging) and the hat ($\hat{\ }$) indicates association with the center. The subscript "f" will later be used to describe the final state.

The total energy of any radially symmetric lens-like eddy is,

$$E = 2\pi\rho \int_0^b \int_0^h (v_\theta^2/2 + g'z)\,r\,dr\,dz \qquad (1.2)$$

where b is the radius of the eddy. For a zero potential vorticity eddy, (1.2) gives,

$$E_i = \pi f^4 b_i / 192g' \qquad . \qquad (1.3)$$

The volume of each vortex (Q) is found to be,

$$Q = \pi f^2 b_i^4 / 16g' \qquad . \qquad (1.4)$$

For an interaction where potential vorticity is conserved, the final energy of the merged vortices is, $\pi f^4 b_f^6 / 192g'$. Here, b_f is the final radius which, from the volume conservation constraint (1.4), is found to be,

---

[1]For clarity, the definition of symbols is given in both the text and an appendix.

$$b_f = b_i \cdot (2)^{\frac{1}{4}} \tag{1.5}$$

where b_i is the original radius of each individual vortex. It, therefore, follows from (1.3) that the ratio of the total final energy to the sum of the initial individual energies is $(2^{\frac{1}{4}})^6 = \sqrt{2}$.

Consequently, it is concluded that, in order for merging to occur, either energy must be supplied from an outside source, or that <u>potential vorticity is not conserved</u>. In addition, if one accepts the idea that physical systems tend to a state of minimum energy, then the above considerations imply that the eddies' natural tendency is to split rather than merge. It should be pointed out that, since for a zero potential vorticity eddy, $b = (8g'\hat{h})^{\frac{1}{2}}/f$ (where $\hat{h}$ is the central depth), it follows from (1.3) that

$$\hat{h}_f = \sqrt{2}\hat{h}_i \tag{1.6}$$

implying that the depth <u>increases</u> during the merging. As mentioned, these relationships were originally derived by Gill and Griffiths (1981).

For additional studies on eddies interaction the reader is referred to Mied and Lindemann (1984), McWilliams (1983), McWilliams and Zabusky (1982), Overman and Zabusky (1982), Melander et al. (1985), and Christiansen and Zabusky (1973). While being informative, the latter investigations are not directly applicable to the problem at hand because they do not address lens-like eddies. The reader is also referred to the laboratory experiments of Griffiths and Hopfinger (1986a,b) and the analysis of Young (1985) which discuss the interaction of quasi-geostrophic and geostrophic vortices. As pointed out in Nof and Simon (1986), these eddies differ from our vortices because the latter are of finite extent whereas the former are infinite.

b) __Methods__: With the conclusions of Gill and Griffiths (1981) in mind, we shall develop a theory for the merging of two blobs. The general details of the proposed merging mechanism are as follows. Two isolated blobs are initially separated from each other; they are embedded in a lighter (or heavier) infinitely deep layer so that, initially, one vortex does not "feel" the presence of its counterpart. The eddies are then brought together by some mean flow which relaxes after it pushes one vortex against the other. This creates a "figure eight" structure with a mutual boundary along which the depth does not vanish (Fig. 2). We shall see that because of the establishment of such a mutual boundary, the eddies cannot remain separated. "Tentacles" are extended from one vortex to another and merging rapidly occurs.

The essence of the theory is that the potential vorticity is altered during the merging; namely, no external source of energy is required and the final potential vorticity of the merged vortex is not identical to the initial potential vorticity which each vortex has had. The details of our proposed merging mechanism involve two main processes. The first is the way in which each of the two vortices becomes entangled in the "tentacles" of its counterpart and the second is the associated change in the potential vorticity. The former can be explained in terms of relatively simple dynamical considerations whereas the latter is believed to be a result of shock waves which are present during the transient merging process.

Both processes are highly nonlinear; the interfaces of the blobs strike the surface (or bottom) so that the depth variations are of $O(1)$ and the centrifugal acceleration is of the same order as the Coriolis force so that the Rossby number is also of $O(1)$. Because of this and the fact that the general problem is three-dimensional (x, y, t), it is impossible to

describe all its details analytically. It is, however, possible to prove analytically that the formation of tentacles is inevitable; namely, it is possible to show that once a "figure eight" and a mutual boundary are established then each vortex must extend an "arm" around its counterpart (Fig. 3). To show this, one of the vortices is, conceptually, replaced by a solid cylinder and the flow resulting from slightly forcing the cylinder into the remaining eddy is examined. Note that since our model is inviscid it makes no difference whether or not the solid cylinder is rotating.

The main idea behind the above simplification is that both an adjacent eddy and an adjacent cylinder are forcing a mutual boundary along which the depth does not vanish. A similar simplification was used by Nof (1986a) to describe the collision between the Gulf Stream and a warm-core ring. However, there are two important differences between the Nof (1986a) analysis and the present model. The first is that while curvature effects are very important in the present study, they are entirely negligible in the Nof (1986a) case. The second is that in the present case the volume of the fluid surrounding the cylinder is finite whereas in the Nof (1986a) study there is a continuous flow from one area to another. These differences make the present study considerably more difficult than that discussed in Nof (1986a). Despite these differences, many of the techniques used in the above study are also applied here. There is some (but limited) over-lapping between the two articles because an attempt has been made to make the present paper self-contained.

Because of the non-vanishing depth along the area in which the fluid is in direct contact with the cylinder, an intrusion of eddy water along the cylinder's perimeter is established. It propagates in a clockwise manner until it ultimately reaches the eddy on the downstream side. At

this point the intrusion reattaches itself to the eddy and the combined eddy-intrusion flow resembles the shape of a padlock. Because of reattachment the "padlock" flow is steady and, even though the problem is still nonlinear, it is possible to obtain an analytical solution. This can be achieved by using a constraint resulting from integrating the equations representing the torque relative to the center of the cylinder. Much of the analysis and discussion in the paper is devoted to the padlock flow. The mere existence of a non-vanishing padlock flow illustrates that intrusion of eddy water along the cylinder is inevitable. We shall see that, consequently, one is led to the conclusion that interleaving and merging must take place.

This paper is organized as follows. In Section 2 the general structure of the merging process is described in detail; this description is largely qualitative. The simplification of the processes in question and the equations governing the padlock flow are given in Section 3. Section 4 contains the appropriate scaling and Section 5 includes the solution for the padlock flow. The results are discussed in Section 6 and summarized in Section 7. A list of symbols is given in the Appendix.

2. The merging process

Consider again the two isolated blobs shown in Fig. 2. The blobs have uniform density and the slightly lighter fluid in which they are embedded is infinitely deep. Initially, the blobs do not touch each other so that there is no repulsion or attraction. The equations governing the motions

-6-

of blobs on the bottom are equivalent to those governing light blobs on the surface or blobs of intermediate density "sandwiched" between two infinitely deep layers. For convenience, we shall only discuss blobs on the bottom of the ocean but it should be kept in mind that our results are also applicable to upper ocean eddies and eddies at mid-depth.

Suppose now that some mean flow has brought the two eddies together so that the eddies' horizontal projection resembles the "figure eight" shape and a mutual boundary is established (Fig. 2); after this happens the mean flow relaxes. Our initial intuition tells us that the eddies' response to the establishment of such a mutual boundary may simply consist of a localized adjusted flow in the vicinity of point B. However, a close examination of the problem shows that this is not the case. To show this, consider an application of the Bernoulli integral to the streamline connecting point A and B assuming, temporarily, that the flow is steady so that the eddies' response (to the establishment of a mutual boundary) consists indeed of a mere adjustment in the vicinity of point B,

$$u_A^2/2 = u_B^2/2 + g'h_B \quad , \tag{2.1}$$

where u_A is the upstream speed (in the x direction) along the front (point A), and u_B and h_B are the speed and depth at B.

Since h_B is always positive, (2.1) implies that $u_B < u_A$. However, if the steady response is in the manner shown in the lower panel of Fig. 2, as we have temporarily assumed, then continuity implies that there must be some convergence across the line connecting point B and the center of the vortices. This suggests that $u_B > u_A$. The above conditions, required by the continuity equation and the Bernoulli principle, are obviously

incompatible, suggesting that there cannot be a streamline connecting A and B. Instead, it is expected that there will be a band of water flowing around the eddies in a clockwise manner (Fig. 3). In other words, particles moving along the vortex edge (i.e., the front) do not have sufficient energy to rise to point B and, therefore, must go around their adjacent vortex where the fluid is lower.

A formal proof for the inevitable existence of the edge intrusion is given in the following sections with aid of the so-called padlock flow. However, it should be pointed out that for the special case corresponding to $u_A = 0$ (i.e., a vortex with a zero speed along the edge) no proof is really necessary because under such conditions (2.1) can never be satisfied. The establishment of tentacles-like edge intrusions along the rims of both eddies creates a structure similar to that displayed in Fig. 4a. As time goes on the tentacles become longer and longer. Since the volume of each vortex is finite the tentacles will ultimately form a single vortex consisting of two adjacent spirals (Fig. 4b).

By equating the volume of each individual blob to the amount of water drained via the lengthening of the tentacles it is possible to estimate the total merging time. Specifically, suppose that εR_d denotes the distance that each vortex is initially "pushed" into its counterpart (where R_d is the deformation radius which is of the same order as the radius of the eddy) and that $\hat{h}$ denotes the eddy central depth. Also, recall that the intrusion advances in a similar fashion to a gravity current so that the propagation rate is of the order of the Kelvin wave speed $(\varepsilon g'\hat{h})^{\frac{1}{2}}$ [see e.g., Griffiths (1986)]. With the aid of this information, we can now equate the volume of each eddy $[\sim O(R_d^2\hat{h})]$ to the intrusion flux $[\varepsilon R_d,$ the

intrusion width, times the intrusion depth $\sim O(\varepsilon \hat{h})$ and the intrusion propagation speed $\sim O(\varepsilon g' \hat{h})^{\frac{1}{2}}$] multiplied by the merging time (t_m). This gives,

$$t_m \sim O\left(f\varepsilon^{5/2}\right)^{-1} \qquad (2.2)$$

which shows that if the relative distance that each vortex is "pushed" into the other is, say, 0.1 and the Coriolis parameter f is $\sim 10^{-4} \sec^{-1}$, then the merging time is roughly 30 days.

The above processes strongly suggest that merging will indeed take place. There remain, however, two important aspects which need to be addressed. The first is that we still need to prove that the intrusions are indeed inevitable. The second is that we need to clarify the relationship between our proposed merging mechanism and the results of Gill and Griffiths (1981) which show that either an external source of energy is needed for the merging or that potential vorticity cannot be conserved during the merging. The former aspect is discussed in Sections 3-5 whereas the latter is addressed below.

The proposed merging process does not require an external source of energy because the mean flow relaxes after the edges of the vortices touch each other. This aspect of energy supply is supported by an independent study involving laboratory experiments on the coalescence of lens-like eddies [see Nof and Simon (1986)]. Consequently, one concludes that it is the potential vorticity that must be altered during the merging. It is

argued that this alteration is achieved via the action of shock waves[2] in the nose of the intrusion. The fact that intrusions contain shock waves is not new. It was first pointed out by Benjamin (1968) for nonrotating flows. The laboratory experiments of Stern et al. (1982), Griffiths and Hopfinger (1983), and Kubokawa and Hanawa (1984), and the analysis presented by Simpson (1982) and Griffiths (1986) suggest that rotating intrusions along straight coastlines also contain shock waves.

Also, the study of Nof (1986c) has demonstrated that the absence of shock waves in an intrusion along a coast is only possible under special conditions. That is, it has been demonstrated that steadily propagating solutions which do not involve shock waves (i.e., the steepening of the intrusions head is arrested by the surrounding flow) are only possible for specific circumstances. These special solutions are not the most general solution to the problem; the general solutions should involve steepening and dissipation associated with depth discontinuities. In an independent study, Nof (1986b) has demonstrated that rotating shock waves cause a major alteration of potential vorticity. We, therefore, suggest that, as the fluid is intruding along the adjacent vortex edge, its potential vorticity is altered. Note that, during the merging, all the fluid in the vortices is intruding so that the potential vorticity of all the fluid is altered. Unfortunately, the detailed analysis of the shocks in the intrusion is quite complicated. It is beyond the scope of this study and will be the subject of a future investigation.

---

[2]By "shock waves" we mean organized depth discontinuities in which there is a violent turbulent action. They correspond to a balance between steepening and dissipative effects.

The above considerations imply that it is not appropriate to assume that potential vorticity is conserved as was done in Gill and Griffiths (1981). In a similar fashion to the energy supply consideration, this conclusion is supported by the laboratory experiments of Nof and Simon (1986). As we saw earlier (Section 1), if one assumes that potential vorticity is conserved during the merging, then one arrives at the result that the central final depth $(\hat{h}_f)$ is <u>larger</u> than the central initial depth [see Eq. (1.6)]. The laboratory experiments of Nof and Simon (1986) show, on the other hand, that this is clearly not the case. In fact, it has been found that the central depth <u>decreases</u> during the merging; for most of the laboratory experiments the final central depth was about <u>half</u> of the initial depth. This completes our qualitative description of the merging processes.

3. The steady "padlock" flow — governing equations and constraints

The present section has two aims. First, we want to show that the eddy's response to the presence of the cylinder cannot consist of a mere adjustment in the contact area (Fig. 5). Namely, we wish to prove that there must always be a flow around the cylinder so that the time dependent intrusion (Fig. 6a) is inevitable. The second aim is to find how the eddy responds to the forced cylinder. Specifically, one would like to compute the padlock flow speed, width and depth as a function of the distance that the cylinder is pushed into the eddy. Because of the inherent nonlinearity of the problem, which has not been removed by our simplification, it is unlikely that one will be able to find analytical solutions for the whole

field. Consequently, we shall make an attempt to find the desired flow pattern without solving for the entire field.

a. <u>General description</u>: Consider the system shown in Fig. 6b. The origin of our coordinates system is located at the center of the cylinder; it will become clear later that this choice is not arbitrary. The x axis is perpendicular to the line connecting the center of the cylinder with the center of the vortex; the y axis is a continuation of the above line and the system rotates uniformly at $f/2$ about the z axis. The padlock flow is embedded in an infinitely deep motionless layer; its potential vorticity is zero. The way that the padlock flow is formed is not important for our analysis. It is useful to point out, however, that one can think of several ways by which it can be established. An obvious procedure is to physically force the cylinder into an eddy. Another method is to, conceptually, pull out a long tube (containing heavy fluid which is not, necessarily, at rest) in the neighborhood of a solid cylinder. The collapse of the fluid initially contained in the tube should take place in a particular location. Specifically, in the absence of the adjacent solid cylinder, the edge of the formed lens should extend beyond the surface of the solid cylinder.

Whatever generation method is used, there will be some period of adjustment during which the lens depth would presumably shrink somewhat to accommodate for the volume of the intrusion around the cylinder. Ultimately, a steady flow will be established and this final steady flow is the focus of our study. At this final stage (Fig. 6b) the boundary of the solid cylinder extends beyond the boundary of a zero potential vorticity eddy whose depth and center are aligned with those of the padlock flow. We

-12-

define this latter vortex to be our "undisturbed" eddy; note that this eddy
is not identical to the initial lens due to the time dependent processes.
Additional comments regarding the differences between the two states are
made in Section 5h.

As stated, the manner in which the padlock flow is established is not
important for the present analysis. What we wish to find out is whether or
not the final adjusted state can only be associated with a padlock flow.
Namely, we ask the following question: Is there a solution corresponding
to a mere adjustment in the contact area? The answer to the latter ques-
tion would be positive if the width of the padlock flow turns out to be
zero. We shall see that this is _not_ the case; i.e., we shall see that
there must be a flow around the cylinder whenever the edge of the undis-
turbed vortex extends beyond the surface of the cylinder ($\varepsilon \neq 0$).

b. <u>Governing equations for regions 1, 2 and 3</u>: The governing equations
for the final adjusted state are the usual shallow water equations. For a
padlock flow with zero potential vorticity we have,

$$\partial v_i/\partial x - \partial u_i/\partial y + f = 0 \quad ; \quad i = 1, 2, 3 \qquad (3.1a)$$

$$u_i \frac{\partial v_i}{\partial x} + v_i \frac{\partial v_i}{\partial y} + f u_i = -g' \frac{\partial h_i}{\partial y} ; \quad i = 1, 2, 3 \qquad (3.1b)$$

$$\frac{\partial}{\partial x} \left(h_i u_i \right) + \frac{\partial}{\partial y} \left(h_i v_i \right) = 0 \quad ; \quad i = 1, 2, 3 \qquad (3.1c)$$

where u and v are the horizontal depth-independent velocity components in
the x and y direction, and the subscripts "1", "2" and "3" denote that the
variable in question is associated with regions 1, 2 and 3 respectively.
Note that because of the symmetry of the problem (i.e., $v = 0$; $h_x = 0$ along

-13-

cross-sections 1, 2 and 3) the x momentum equation $\left(\dfrac{\partial u_i}{\partial x} + v_i \dfrac{\partial u_i}{\partial y} - fv_i = \right.$ $\left. -g' \dfrac{\partial h}{\partial x} \right)$ and the continuity equation (3.1c) imply that,

$$\frac{\partial u_i}{\partial x} = 0 \qquad\qquad (3.2)$$

In addition, note that, as in many radially symmetric eddies, $\dfrac{\partial v_i}{\partial x}$ is <u>not</u> necessarily zero where $x = 0$ even though $v = 0$.

The boundary conditions for regions 1, 2 and 3 are,

$$h_1 = 0 \quad ; \quad y = -r_0(1 - \epsilon) - 4\sqrt{2} \cdot R_d - 2\sqrt{2} \cdot R_d(1 - \gamma_1) \qquad (3.3a)$$

$$h_1 = \hat{h} \quad ; \quad y = -r_0(1 - \epsilon) - 2\sqrt{2} \cdot R_d \qquad\qquad (3.3b)$$

$$u_1 = v_1 = 0 \quad ; \quad y = -r_0(1 - \epsilon) - 2\sqrt{2} \cdot R_d \qquad\qquad (3.3c)$$

$$\left[u_1{}^2 \right]_{y \ = \ -r_0(1 - \epsilon) - 2\sqrt{2} \cdot R_d(2 - \gamma_1)} = \left[u_3{}^2 \right]_{y \ = \ r_0(1 + \gamma_3)} \qquad (3.4)$$

$$\left[u_2{}^2 + 2g'h_2 \right]_{y \ = \ -r_0} = \left[u_3{}^2 + 2g'h_3 \right]_{y \ = \ r_0} \qquad (3.5a)$$

$$h_2 = \hat{h} \quad ; \quad y = -r_0(1 - \epsilon) - 2\sqrt{2} \cdot R_d \qquad\qquad (3.5b)$$

$$u_2 = v_2 = 0 \quad ; \quad y = -r_0(1 - \epsilon) - 2\sqrt{2} \cdot R_d \qquad\qquad (3.5c)$$

$$h_3 = 0 \quad ; \quad y = r_0(1 + \gamma_3) \quad , \qquad\qquad (3.6)$$

where r_0 is the radius of the cylinder and R_d is the deformation radius based on the depth at the center of the padlock flow (i.e., where the speed vanishes) so that the radius of the undisturbed vortex is $2\sqrt{2} \cdot R_d$. γ_1 and γ_3 denote the nondimensional locations at which the depths of the flow in

regions 1 and 3 vanish. Conditions (3.3a) and (3.6) state that the depth of these flows vanishes at some unknown location; conditions (3.4) and (3.5a) reflect the conservation of energy along the streamlines that bound the flow from left and right (looking downstream). Namely, (3.4) and (3.5a) are simply a result of an application of the Bernoulli integral to the streamlines connecting G and E, and B and D (see Fig. 6b). Conditions (3.3b) and (3.5b) state that at A the depths of the two regions are identical to some given depth (ħ) and (3.3c) and (3.5c) reflect the requirement for a vanishing speed at the center of the vortex.

It is important to clearly distinguish between the undisturbed state and the initial state. As mentioned before, the undisturbed vortex is defined as a zero potential vorticity vortex which is centered at the center of the padlock flow (i.e., the point where the velocity vanishes) and has the same depth as the maximum padlock flow (ħ); its radius is $2\sqrt{2} \cdot R_d$. The initial state, on the other hand, is the state which leads to the intrusion and the padlock flow — it is of no interest for the present study.

c. <u>Constraints</u>: The flows in the various regions are connected to each other via (3.4) and (3.5) but there are two additional constraints that the unknown variables must satisfy. The first results simply from continuity and can be written in the form,

$$\int_{G}^{A} u_1 h_1 dy \quad + \quad \int_{A}^{B} u_2 h_2 dy \quad + \quad \int_{D}^{E} u_3 h_3 dy \quad = 0 \qquad (3.7)$$

The second equation will be derived from the conservation of torque. As in Nof (1986a), we begin by noting that the moment of momentum corresponds to the cross-product of the position vector r and the momentum equations,

$$y \left(u \frac{\partial u}{\partial x} + v \frac{\partial u}{\partial y} - fv + g' \frac{\partial h}{\partial x} \right) - x \left(u \frac{\partial v}{\partial x} + v \frac{\partial v}{\partial y} + fu + g' \frac{\partial h}{\partial y} \right) = 0 . \tag{3.8}$$

To show that (3.8) provides an additional connection between regions 1, 2 and 3, it is multiplied by h and the continuity equation (3.7a) is incorporated. This gives,

$$\frac{\partial}{\partial x} (hu^2y) + y \frac{\partial}{\partial y} (huv) - fvyh + \frac{g'}{2} \frac{\partial}{\partial x} (h^2y)$$

$$- x \frac{\partial}{\partial x} (huv) - \frac{\partial}{\partial y} (hxv^2) - fuhx - \frac{g'}{2} \frac{\partial}{\partial y} (h^2x) = 0 \quad , \tag{3.9}$$

which can be rearranged and integrated over the region shown in Fig. 7, to give,

$$\int\!\!\!\int_{-\infty}^{+\infty} \frac{\partial}{\partial x} \left(hu^2y - f\psi y + \frac{g'}{2} h^2y - huvx \right) dxdy$$

$$+ \int\!\!\!\int_{-\infty}^{+\infty} \frac{\partial}{\partial y} \left(huvy + f\psi x - \frac{g'}{2} h^2x - hxv^2 \right) dxdy = 0 \tag{3.10}$$

where ψ is a stream function defined by,

$$\frac{\partial \psi}{\partial y} = -uh \quad ; \quad \frac{\partial \psi}{\partial x} = vh \quad . \tag{3.11}$$

By using Stokes' theorem, (3.11) can be written in the form,

-16-

$$\oint_{\phi} \left(hu^2y - f\psi y + \frac{g'}{2} h^2y - huvx \right) dy$$

$$-\oint_{\phi} \left(huvy - hxv^2 + f\psi x - \frac{g'}{2} h^2x \right) dx \quad . \qquad (3.12)$$

where ϕ is the boundary of the flow. This equation can be further simpli-fied by defining ψ to be zero along the edge where h = 0 and noting that along any streamline udy = vdx. This gives,

$$\int_{G}^{B} \left(hu^2 - f\psi + g'h^2/2 \right) ydy + \int_{D}^{E} \left(hu^2 - f\psi + g'h^2/2 \right) ydy$$

$$+ \int_{B}^{D} \left(-f\psi y + g'h^2y/2 \right) dy - \int_{B}^{D} \left(f\psi x - g'h^2x/2 \right) dx = 0 \quad (3.13)$$

In deriving (3.13) it has been taken into account that the sum of the integrals of hu^2y and huvy along BD vanishes because there is no normal flow through the boundary of the cylinder.

The first two terms in (3.13) are the moments of the flow force in regions 1, 2 and 3. The last two terms, on the other hand, represent the torque corresponding to the pressure exerted on the cylinder by the sur-rounding flow. Since we chose our origin to be in the center of the cylinder and the pressure is always perpendicular to the surface with which the fluid is in contact, we would expect this torque to vanish. It is easy to show that since the cylinder surface is given by $x^2 + y^2 = r_0^2$, we have xdx + ydy = 0 so that the sum of the last two integrals in (3.13) equals zero as expected. Hence, the integrated torque takes the simple form,

$$\int_G^A \left(h_1 u_1{}^2 - f\psi_1 + g'h_1{}^2/2 \right) y\, dy + \int_A^B \left(h_2 u_2{}^2 - f\psi_2 + g'h_2{}^2/2 \right) y\, dy$$

$$+ \int_D^E \left(h_3 u_3{}^2 - f\psi_3 + g'h_3{}^2/2 \right) y\, dy = 0 \ , \quad (3.14)$$

where we have incorporated our special notation for the various regions. Note that (3.14) does not involve any variables other than those of regions 1, 2 and 3.

4.   **Scaling and expansion of the padlock flow**

a)   <u>The basic state</u>: Before discussing the scaling of the problem and the general structure of the expansion, it is instructive to look at the details of the basic state. The structure of the zeroth order state, corresponding to the cylinder "kissing" an eddy with zero potential vorticity, is not <u>a priori</u> obvious. To show this, consider the application of the Bernoulli integral to the surface of the cylinder (3.5). It implies that even when $\varepsilon \to 0$ the velocity along the cylinder surface is of $O(1)$ because the eddy speed along the edge is $O(1)$ [see (1.1) with $r = 2(2g'\hat{h})^{\frac{1}{2}}/f$]. As in Nof (1986a), this means that the basic flow around the cylinder is not zero; rather, it consists of an infinitesimal ribbon flowing at a speed $(2g'\hat{h})^{\frac{1}{2}}$. To find the details of this ribbon flow it is noted that even though the basic state contains only an infinitesimal strip, it must, of course, satisfy the equations of motion.

-18-

It is convenient to consider the potential vorticity equation and momentum conservation in cylindrical coordinate (r, θ),

$$\frac{1}{r} \frac{d}{dr} \left(r\overline{v_\theta} \right) + f = 0 \qquad (4.1)$$

$$\frac{\overline{v_\theta}^2}{r} + f\overline{v_\theta} = g' \frac{\overline{dh}}{dr} \qquad , \qquad (4.2)$$

where $\overline{v_\theta}$ is the tangential velocity, the bar $(-)$ indicates association with the basic state and we have assumed that the basic flow is purely tangential (i.e., $\overline{v_r} = \frac{\partial}{\partial \theta} = 0$). The most general solution of (4.1) and (4.2) is,

$$\overline{v_\theta} = -\frac{fr}{2} + \frac{\alpha}{r} \quad ; \quad \overline{h} = \left(r_0^2 - r^2 \right) \frac{f^2}{8g'} + \left(\frac{1}{r_0^2} - \frac{1}{r^2} \right) \frac{\alpha^2}{2g'} \quad , \quad (4.3)$$

where α is an unknown constant and we have used the condition $\overline{h} = 0$ at $r = r_0$. Since at $r = r_0$ the absolute value of the velocity must be $(2g'\overline{h})^{\frac{1}{2}}$ (in order to satisfy the Bernoulli relationship along the surface of the cylinder), we find from (4.3) that,

$$\alpha = \frac{fr_0}{2} \left(r_0 - 2(2)^{\frac{1}{2}} R_d \right) \qquad (4.4)$$

where $R_d = (g'\overline{h})^{\frac{1}{2}}/f$. Namely, for any given cylinder (r_0), we must take a specific value for α. For simplicity, we shall consider only cylinders with $r_0 = 2(2)^{\frac{1}{2}} R_d$ so that $\alpha = 0$. Other cylinders can, of course, also be considered and the solution, which will be shortly derived, can be easily

-19-

extended to cylinders with all diameters. However, such extended solutions
do not provide any new physical insights and, therefore, are not presented.

b) <u>Scaling</u>: In the subsequent analysis the following nondimensional
variables will be used,

$$
u^* = u/(g'\hat{h})^{\frac{1}{2}} \quad ; \quad v^* = v/(g'\hat{h})^{\frac{1}{2}} \quad ; \quad h^* = h/\hat{h}
$$

$$
\left. \begin{array}{l}
x^* = x/R_d \quad ; \quad y^* = y/R_d \quad ; \quad r_0^* = r_0/R_d = 2(2)^{\frac{1}{2}} \quad ; \quad r^* = r/R_d \\
\\
\psi^* = \psi/[g'(\hat{h})^2/f] \quad ; \quad R_d = (g'\hat{h})^{\frac{1}{2}}/f
\end{array} \right\} \quad (4.5)
$$

Note that in regions 1 and 3, which are located far from the contact area,
the flow is taken to be purely tangential. In region 2, however, some
deviations from radially symmetric motion are possible because of the
presence of the cylinder. In view of this, we shall use polar coordinates
for regions 1 and 3 and Cartesian coordinates for region 2. [The subscript θ
will denote association with polar coordinates (i.e., v_θ is the azimuthal
speed) whereas the lack of a subscript will indicate that the variable in
question is associated with Cartesian coordinates.] For region 1 it is
convenient to transfer the coordinate system and use cylindrical coordi-
nates ($\tilde{r}$, $\tilde{\theta}$) centered at the center of the padlock flow $[0; -r_0(2 - \epsilon)]$.
In terms of the nondimensional numbers defined by (4.5), the governing
equations for this region are,

$$
\frac{1}{\tilde{r}} \frac{d}{d\tilde{r}} (\tilde{r} \, \tilde{v}_{\theta 1}) + 1 = 0 \quad ; \quad (\tilde{v}_{\theta 1})^2/\tilde{r} + \tilde{v}_{\theta 1} = \frac{d\tilde{h}_1}{d\tilde{r}} \quad (4.6a)
$$

-20-

where $\tilde{r}$, $\tilde{\theta}$ are related to the original coordinates system (x^*, y^*) via,

$$\tilde{r}\sin\tilde{\theta} = y^* + 2(2)^{\frac{1}{2}}(2 - \epsilon) \quad ; \quad \tilde{r}\cos\tilde{\theta} = x^* \qquad (4.6b)$$

[i.e., $\tilde{y} = y^* + 2\sqrt{2}(2 - \epsilon)$; $\tilde{x} = x^*$]. For region 3 it is not advantageous to transfer the coordinates system. We, therefore, take,

$$\frac{1}{r^*}\frac{d}{dr^*}(r^* v_{\theta_3}^*) + 1 = 0 \quad ; \quad (v_{\theta_3}^*)^2/r^* + v_{\theta_3}^* = \frac{dh_3^*}{dr^*} \qquad (4.6c)$$

The nondimensional equations for region 2 are found from (4.5) and (3.1) to be,

$$\frac{\partial v_2^*}{\partial x^*} - \frac{\partial u_2^*}{\partial y^*} + 1 = 0 \qquad (4.7a)$$

$$u_2^*\frac{\partial v_2^*}{\partial x^*} + u_2^* = -\frac{\partial h_2^*}{\partial y^*} \qquad (4.7b)$$

$$\frac{\partial}{\partial x^*}(h_2^* u_2^*) = 0 \qquad (4.7c)$$

where we have taken into account that $v_2^* = 0$ because of symmetry. Note, however, that, as mentioned before, the terms containing $\partial v_2^*/\partial x^*$ are not necessarily zero even though $v_2^* = 0$. The boundary conditions (3.3 - 3.6) take the form,

$$h_1^* = 0 \quad ; \quad y^* = -2(2)^{\frac{1}{2}}(3 - \epsilon - \gamma_1) \qquad (4.8a)$$

$$h_1^* = 1 \quad ; \quad y^* = -2(2)^{\frac{1}{2}}(2 - \epsilon) \qquad (4.8b)$$

$$u_1^* = v_1^* = 0 \quad ; \quad y^* = -2(2)^{\frac{1}{2}}(2 - \epsilon) \qquad (4.8c)$$

$$\left[(u_1^*)^2\right]_{y^* = -2(2)^{\frac{1}{2}}(3 - \varepsilon - \gamma_1)} = \left[(u_3^*)^2\right]_{y^* = 2(2)^{\frac{1}{2}}(1 + \gamma_3)} \quad (4.9)$$

$$\left[(u_2^*)^2 + 2h_2^*\right]_{y^* = -2(2)^{\frac{1}{2}}} = \left[(u_3^*)^2 + 2h_3^*\right]_{y^* = 2(2)^{\frac{1}{2}}} \quad (4.10a)$$

$$h_2^* = 1 \quad ; \quad y^* = -2(2)^{\frac{1}{2}}(2 - \varepsilon) \quad (4.10b)$$

$$u_2^* = v_2^* = 0 \quad ; \quad y^* = -2(2)^{\frac{1}{2}}(2 - \varepsilon) \quad (4.10c)$$

$$h_3^* = 0 \quad ; \quad y^* = 2(2)^{\frac{1}{2}}(1 + \gamma_3) \quad (4.11)$$

Similarly, the constraints (3.7) and (3.14) can be expressed as,

$$\int_{-2(2)^{\frac{1}{2}}(3 - \varepsilon - \gamma_1)}^{-2(2)^{\frac{1}{2}}(2 - \varepsilon)} u_1^* h_1^* dy + \int_{-2(2)^{\frac{1}{2}}(2 - \varepsilon)}^{-2(2)^{\frac{1}{2}}} u_2^* h_2^* dy^* + \int_{2(2)^{\frac{1}{2}}}^{2(2)^{\frac{1}{2}}(1 + \gamma_3)} u_3^* h_3^* dy^* = 0 \quad (4.12)$$

and,

$$\int_{-2(2)^{\frac{1}{2}}(3 - \varepsilon - \gamma_1)}^{-2(2)^{\frac{1}{2}}(2 - \varepsilon)} \left[h_1^*(u_1^*)^2 - \psi_1^* + (h_1^*)^2/2\right]y^* dy^* + \int_{-2(2)^{\frac{1}{2}}(2 - \varepsilon)}^{-2(2)^{\frac{1}{2}}} \left[h_1^*(u_2^*)^2 - \psi_2^* + (h_2^*)^2/2\right]y^* dy^*$$

$$+ \int_{-2(2)^{\frac{1}{2}}}^{-2(2)^{\frac{1}{2}}(1 + \gamma_3)} \left[h_3^*(u_3^*)^2 - \psi_3^* + (h_3^*)^2/2\right]y^* dy^* = 0$$

$$(4.13)$$

c) <u>Perturbation expansion</u>: As in Nof (1986a), the expansion in ε is not straightforward for two reasons. First, as already pointed out, the basic state ($\varepsilon = 0$) contains speeds of $O(1)$. Secondly, the choice for the origin

of the coordinates system implies that the basic flow is a function of ε.
Recall that the choice of the origin for the coordinate system was "im-
posed" by the use of the integrated torque. If the origin were in any
other location, then the integrated torque associated with the pressure
along BCD would have remained nonzero thus making it impossible to connect
the three regions. It will become clear shortly that while these condi-
tions make the expansion somewhat more involved they do not present any
fundamental difficulty.

It is assumed that, for regions 1 and 3, the expansion has the form,

$$\tilde{v}_{\theta 1} = -\tilde{r}/2 + \varepsilon \tilde{v}_{\theta 1}^{(1)} + \varepsilon^2 \tilde{v}_{\theta 1}^{(2)} + \ldots \tag{4.14a}$$

$$\tilde{h}_1 = 1 - (\tilde{r})^2/8 + \varepsilon \tilde{h}_1^{(1)} + \varepsilon^2 \tilde{h}_1^{(2)} + \ldots \tag{4.14b}$$

$$\gamma_1 = \varepsilon \gamma_1^{(1)} + \varepsilon^2 \gamma_1^{(2)} + \ldots \tag{4.14c}$$

$$v_{\theta 3}^* = -r^*/2 + \varepsilon v_{\theta 3}^{(1)} + \varepsilon^2 v_{\theta 3}^{(2)} + \ldots \tag{4.15a}$$

$$h_3^* = 1 - (r^*)^2/8 + \varepsilon h_3^{(1)} + \varepsilon^2 h_3^{(2)} + \ldots \tag{4.15b}$$

$$\gamma_3 = \varepsilon \gamma_3^{(1)} + \varepsilon^2 \gamma_3^{(2)} + \ldots \quad , \tag{4.15c}$$

where (4.3) and (4.5) have been used to express the terms corresponding to
the basic state. Note that, as before, the tilde ($\tilde{\ }$) denotes association
with a polar coordinates system whose origin is located at the center of
the eddy instead of the center of the cylinder ($x^* = y^* = 0$). The rela-
tionship between $\tilde{r}$ and x^* and y^* is easily found from (4.6b) to be,

$$\tilde{r} = \left\{ (x^*)^2 + [y^* + 2(2)^{\frac{1}{2}} (2 - \varepsilon)]^2 \right\}^{\frac{1}{2}} \quad . \qquad (4.15d)$$

As in Nof (1986a), the expansions (4.14 - 4.15) take into account that the width of the flow around the cylinder (γ_3) is $O(\varepsilon R_d)$ because this is also the width of the flow blocked by the cylinder (i.e., section BB', Fig. 6b). In other words, the width of the flow in region 3 is of the order of the distance that the cylinder is "pushed" into the eddy. The depth near the cylinder boundary in region 3 must be of the same order as the depth at B because the blocked transport is $O(g'h_B^2/2f)$ and the transport at cross-section 3 is $O(g'h_{3w}^2/2f)$ [where h_{3w} is the depth near the wall at region 3]. Namely, a Taylor series expansion (around the edge of the undisturbed eddy) for the depth at B shows that $h_B \sim O(\varepsilon\hbar)$ and, consequently, $h_{3w} \sim O(\varepsilon\hbar)$. These scales are consistent with the scales that one finds along the immediate vicinity of the rim of any lens-like eddy.

As mentioned, in region 2 the flow is not necessarily radially symmetric so that the expansion is,

$$u_2^* = \left[y^* + 2(2)^{\frac{1}{2}} (2 - \varepsilon)\right]/2 + \varepsilon u_2^{(1)} + \varepsilon^2 u_2^{(2)} + . . . \qquad (4.16a)$$

$$v_2^* = -x^*/2 + \varepsilon v_2^{(2)} + \varepsilon^2 v_2^{(2)} + . . . \qquad (4.16b)$$

$$h_2^* = 1 - \left[y^* + 2(2) (2 - \varepsilon)\right]^2/8 + \varepsilon h_2^{(1)} + \varepsilon^2 h_2^{(2)} + . . . \qquad (4.16c)$$

Recall now that because of our choice for the origin of (x^*, y^*), our basic state contains ε when it is expressed in terms of x^* and y^*. While this does not create any difficulties, it is perhaps more appropriate to express (4.16a) and (4.16c) in the form,

-24-

$$u_2* = \left[y* + 4(2)^{\frac{1}{2}}\right]/2 + \varepsilon\left(u_2^{(1)} - (2)^{\frac{1}{2}}\right) + \varepsilon^2 u_2^{(2)} + \ldots \qquad (4.17a)$$

$$h_2* = 1 - \left(y* + 4(2)^{\frac{1}{2}}\right)^2/8 + \varepsilon\left(h_2^{(1)} + y*(2)^{\frac{1}{2}}/2\right) + \varepsilon^2\left(h_2^{(2)} - 1\right) \ldots \quad (4.17b)$$

In this form, the power series are expressed in a way that clearly separates the zeroth-order terms from the remaining terms. Hereafter, the first terms in (4.17) will be referred to as $u_2^{(0)}$ and $h_2^{(0)}$, respectively.

5. Solution for the padlock flow

a) <u>General solution for region 1</u>: Substitution of (4.14) into (4.6) and elimination of the terms corresponding to the basic state[3] gives the $0(\varepsilon)$ equation,

$$\frac{1}{\tilde{r}} \frac{d}{d\tilde{r}} \left(\tilde{r} \, \tilde{v}_{\theta 1}^{(1)} \right) = 0 \qquad (5.1)$$

The solution is: $\tilde{v}_{\theta 1}^{(1)} = A_1/\tilde{r}$, where A_1 is an unknown constant. Since $\tilde{v}_\theta^{(1)}$ cannot approach infinity at the center of the vortex ($\tilde{r} = 0$) we find that,

$$\tilde{v}_{\theta 1}^{(1)} = A_1 = 0 \qquad (5.2)$$

---

[3]Recall that the zeroth-order state was defined as a zero potential vorticity vortex with a depth identical to the maximum padlock flow depth. It is centered where the orbital speed of the padlock flow vanishes. Namely, when $\varepsilon = 0$, the basic vortex is kissing the cylinder.

and $\tilde{h}_1{}^{(1)} = B_1$ where B_1 is a constant to be determined. At the center of the vortex the depth $\tilde{h}$ must match the undisturbed depth ($\tilde{h} = 1$) because of our definition of the basic state. Hence, we have $B_1 = 0$ and

$$\tilde{h}_1{}^{(1)} = 0 \qquad (5.3a)$$

Also, with the aid of (4.8a) one obtains,

$$\tilde{\gamma}_1{}^{(1)} = 0 \qquad (5.3b)$$

It is a simple matter to show that, in a similar fashion to the first-order solution, the second-order solution in region 2 also vanishes, i.e.,

$$\tilde{h}_1{}^{(2)} = \tilde{v}_{\theta 1}{}^{(2)} = \gamma_1{}^{(2)} = 0 \qquad . \qquad (5.3c)$$

b) <u>Simplified equations for region 2</u>: From (4.16) and (4.7) one finds the $O(\varepsilon)$ equations,

$$\frac{\partial v_2{}^{(1)}}{\partial x^*} - \frac{\partial u_2{}^{(1)}}{\partial y^*} = 0 \qquad (5.4a)$$

$$u_2{}^{(0)} \frac{\partial v_2{}^{(1)}}{\partial x^*} + u_2{}^{(1)}/2 = -\frac{\partial h_2{}^{(1)}}{\partial y^*} \qquad (5.4b)$$

$$\frac{\partial}{\partial x^*} \left[\left(1 - (y^*)^2/8\right)u_2{}^{(1)} + h_2{}^{(1)}/2 \right] = 0 \qquad (5.4c)$$

-26-

The $O(\varepsilon^2)$ balances are,

$$\frac{\partial v_2^{(2)}}{\partial x^*} - \frac{\partial u_2^{(2)}}{\partial y^*} = 0 \qquad (5.5a)$$

$$u_2^{(1)} \frac{\partial v_2^{(1)}}{\partial x^*} + \frac{\partial v_2^{(2)}}{\partial x^*} \left(\frac{y^*}{2}\right) - u_2^{(2)}/2 + u_2^{(2)} = -\frac{\partial h_2^{(2)}}{\partial y^*} \qquad (5.5b)$$

$$\frac{\partial}{\partial x^*} \left\{ h_2^{(2)} y^*/2 + h_2^{(1)} u_2^{(1)} + \left[1 - (y^*)^2/8\right] u_2^{(2)} \right\} = 0 \qquad (5.5c)$$

The geometry of the region in the immediate vicinity of region 2 is shown in Fig. 8.

c) <u>General solution for region 3</u>: By substituting (4.15) into (4.6c) and eliminating the basic state, one obtains the equations,

$$\frac{\varepsilon}{r^*} \frac{d}{dr^*} \left[r^* v_{\theta3}^{(1)} + \varepsilon r^* v_{\theta3}^{(2)} \right] + O(\varepsilon^3) = 0 \qquad (5.7)$$

$$0 = \varepsilon \frac{dh_3^{(1)}}{dr^*} \qquad (5.8)$$

It will become clear shortly that the term containing $v_{\theta3}^{(2)}$ is actually $O(\varepsilon)$ and not $O(\varepsilon^2)$ so that it must be included in the $O(\varepsilon)$ balance.

To simplify the structure of (5.7), it is recalled that the first-order flow (in region 3) takes place within a distance of $O(\varepsilon)$ from the cylinder surface so that, as in Nof (1986a), one may introduce the transformation,

$$r^* = 2(2)^{\frac{1}{2}}(1 + \varepsilon \xi^*) \quad , \quad \text{where } \xi^* - 0(1) \ .$$

In terms of this new variable, (5.7) is,

$$\frac{1}{2(2)^{\frac{1}{2}}} \frac{dv_{\theta_3}{}^{(1)}}{d\xi^*} + \varepsilon \left[\frac{\xi^*}{2(2)^{\frac{1}{2}}} \frac{dv_{\theta_3}{}^{(1)}}{d\xi^*} + v_{\theta_3}{}^{(2)} \right] + 0(\varepsilon^2) = 0$$

which shows that $dv_{\theta_3}{}^{(1)}/d\xi^* = 0$. This and (5.8) give,

$$v_{\theta_3}{}^{(1)} = B_3 \quad ; \quad h_3{}^{(1)} = A_3 \tag{5.9}$$

where B_3 and A_3 are constants to be determined from the boundary conditions. Substitution of (5.9), (4.15), (5.2), (5.3) and (4.14) into the polar version of the boundary conditions (4.9) and (4.11) gives,

$$\left[-\tilde{r}/2 \right]_{\tilde{r}\,=\,2(2)^{\frac{1}{2}}(1\,+\,\varepsilon\gamma_1{}^{(1)})}^{2} = \left[-r^*/2 + \varepsilon B_3 \right]_{r^*\,=\,2(2)^{\frac{1}{2}}\left(1\,+\,\varepsilon\gamma_3{}^{(1)}\right)}^{2} \tag{5.10}$$

$$\left[1 - (r^*)^2/8 \right] + \varepsilon A_3 = 0 \quad ; \quad r^* = 2(2)^{\frac{1}{2}}\left(1 + \varepsilon\gamma_3{}^{(1)}\right) \tag{5.11}$$

which, with the aid of (5.3b), yields,

$$B_3 = (2)^{\frac{1}{2}}\gamma_3{}^{(1)} \quad ; \quad A_3 = 2\gamma_3{}^{(1)} \tag{5.12}$$

By now, most of the first-order solution for region 3 has been derived; the only part that is still missing is $\gamma_3{}^{(1)}$. As we shall see, there are two equations and a boundary condition (4.10a) which we have not used yet. The latter immediately gives,

$$(2)^{\frac{1}{2}}u_2{}^{(1)} = h_2{}^{(1)} \quad \text{at } y^* = -2(2)^{\frac{1}{2}} \quad . \tag{5.13}$$

-28-

d) **The torque constraint:** Since $(h_3^*) \sim O(\gamma_3) \sim O(\varepsilon)$ it follows that the third integral in (4.13) is, at the most, $O(\varepsilon^2)$. With the aid of the transformation $\tilde{y} = y^* + 2(2)^{\frac{1}{2}}(2 - \varepsilon)$ and (5.3b), the approximate form of (4.13) [up to $O(\varepsilon^2)$] can be rewritten as,

$$\int_{-2(2)^{\frac{1}{2}}}^{0} \left[\tilde{h}_1(\tilde{u}_1)^2 - \tilde{\psi}_1 + (\tilde{h}_1)^2/2\right] \left[\tilde{y} - 2(2)^{\frac{1}{2}}(2 - \varepsilon)\right] d\tilde{y}$$

$$+ \int_{0}^{2(2)^{\frac{1}{2}} - \varepsilon} \left[\tilde{h}_2(\tilde{u}_2)^2 - \tilde{\psi}_2 + (\tilde{h}_2)^2/2\right] \left[\tilde{y} - 2(2)^{\frac{1}{2}}(2 - \varepsilon)\right] d\tilde{y} + O(\varepsilon^2) = 0 \qquad (5.14)$$

where, as before, the tilde ($\tilde{\ }$) above the variables u, ψ and h indicates that they are expressed in terms of $\tilde{x}$, $\tilde{y}$. Substitution of (4.14), (4.17), (5.2) and (5.3) into (5.14) and elimination of the basic state gives,

$$\int_{0}^{2(2)^{\frac{1}{2}}} \left[2\tilde{h}_2^{(0)}\tilde{u}_2^{(0)}\tilde{u}_2^{(1)} + \left(\tilde{u}_2^{(0)}\right)^2 \tilde{h}_2^{(1)} - \psi_2^{(1)} + \tilde{h}_2^{(0)}\tilde{h}_2^{(1)}\right]\left(\tilde{y} - 4(2)^{\frac{1}{2}}\right) d\tilde{y}$$

$$+ \int_{2(2)^{\frac{1}{2}}}^{2(2)^{\frac{1}{2}} - \varepsilon} \left[\tilde{h}_2^{(0)}\left(\tilde{u}_2^{(0)}\right)^2 - \tilde{\psi}^{(0)} + \left(\tilde{h}_2^{(0)}\right)^2/2\right]\left(\tilde{y} - 4(2)^{\frac{1}{2}}\right) d\tilde{y} + O(\varepsilon^2) = 0$$

$$(5.15)$$

This equation can be further simplified by noting that the second integral is associated with the area where $\tilde{h}_2^{(0)} \sim O(\varepsilon)$, and $\tilde{\psi}_2^{(0)} \sim O(\varepsilon^2)$ so that it is, at the most, of $O(\varepsilon^2)$. Hence, to $O(\varepsilon)$, (5.15) reduces to,

$$\int_0^{2(2)^{\frac{1}{2}}} \left[2\tilde{h}_2^{(0)}\tilde{u}_2^{(0)}\tilde{u}_2^{(1)} + \left(\tilde{u}_2^{(0)}\right)^2\tilde{h}_2^{(1)} - \psi_2^{(1)} + \tilde{h}_2^{(0)}\tilde{h}_2^{(1)}\right]\left(\tilde{y} - 4(2)^{\frac{1}{2}}\right)d\tilde{y}$$

$$+ \, O(\varepsilon^2) = 0$$

which, in terms of the x^*, y^* coordinates, is,

$$\int_0^{-2(2)^{\frac{1}{2}}} \left[2h_2^{(0)}u_2^{(0)}u_2^{(1)} + \left(u_2^{(0)}\right)^2 h_2^{(1)} - \psi_2^{(1)} + h_2^{(0)}h_2^{(1)}\right]y^* dy^* + O(\varepsilon^2) = 0$$

(5.16)

A solution satisfying (5.16), the boundary condition (5.13) and the governing equations (5.4a-c) is simply,

$$u_2^{(1)} = h_2^{(1)} = \psi_2^{(1)} = 0 \tag{5.17}$$

This leaves only one unknown, $\gamma_3^{(1)}$, which will be computed from the $O(\varepsilon^2)$ balances.

The fact that the situation displayed in Fig. 5 is impossible can now be shown even without computing the specific value of $\gamma_3^{(1)}$. To show this suppose, temporarily, that the situation shown in Fig. 5 is possible. Then application of the Bernoulli principle to the streamline associated with eddy edge implies that since the depth perturbation at B is $O(\varepsilon)$, the perturbed velocity along the edge must also be of $O(\varepsilon)$. Relation (5.17)

shows, however, that this is impossible indicating that the streamline associated with the edge cannot pass through point B.

e) <u>The second order balances</u>: Two comments should be made before discussing the $O(\epsilon^2)$ equations. The first is that the $O(\epsilon)$ continuity equation is automatically satisfied by the $O(\epsilon)$ solution that we have derived for region 2. The second is that although the $O(\epsilon^2)$ continuity constraint involves the $O(\epsilon)$ variables in region 3, it also involves the $O(\epsilon^2)$ variables in region 2. In other words, as in Nof (1986a), it is necessary to find the $O(\epsilon^2)$ solution in regions 1 and 2 in order to obtain the $O(\epsilon)$ solution in region 3.

In view of this, we shall consider now the $O(\epsilon^2)$ potential vorticity equation, the momentum balance, and the local continuity balance for region 2 [equations (5.5a-c)] which have the solution,

$$u_2^{(2)} = \delta\bar{y} \quad ; \quad \frac{\partial v_2^{(2)}}{\partial\tilde{x}} = \delta \quad ; \quad h_2^{(2)} = -\delta y^2/2 \qquad (5.18)$$

where δ is a constant to be determined.

This solution satisfies the boundary condition $u_2^{(2)} = v_2^{(2)} = h_2^{(2)} = 0$ at $x^* = y^* = 0$ as required. Together with the first and second-order solutions for the various regions and the second-order solution for region 1 [relation (5.3c)], the second-order balance of the integrated continuity equation gives,

$$1 + 2\delta = \left(\gamma_3^{(1)}\right)^2 \quad . \qquad (5.19a)$$

Similarly, the second-order balance of the integrated torque (4.13) yields,

-31-

$$3.4678 - 3 + \left(\gamma_3{}^{(1)}\right)^2 = 0 \quad . \tag{5.19b}$$

Equations (5.19a) and (5.19b) have the solution,

$$\gamma_3{}^{(1)} = 1.316 \quad ; \quad \delta = 0.366 \tag{5.19c}$$

and this completes the derivation of the solution.

f) **The complete solution:** The total solution for region 1 is,

$$\left.\begin{aligned}
u_1{}^* &= \tilde{y}/2 + 0(\epsilon^3) \\
h_1{}^* &= \left[1 - (\tilde{y})^2/8\right] + 0(\epsilon^3) \\
v_1{}^* &= 0 \\
\gamma_1 &= 0 + 0(\epsilon^3)
\end{aligned}\right\} \tag{5.20a}$$

In terms of the non-transformed coordinates [see (4.6b)], it takes the form,

$$\left.\begin{aligned}
u_1{}^* &= \left(y^* + 4\sqrt{2}\right)/2 - \sqrt{2}\cdot\epsilon + 0(\epsilon^3) \\
h_1{}^* &= \left[1 - \left(y^* + 4\sqrt{2}\right)^2/8\right] + \epsilon\left(y^* + 4\sqrt{2}\right)\sqrt{2}/2 - \epsilon^2 + 0(\epsilon^3) \\
v_1{}^* &= 0 \quad ; \quad \gamma_1 = 0 + 0(\epsilon^3)
\end{aligned}\right\} \tag{5.20b}$$

where, as pointed out earlier, the terms of $0(\epsilon)$ in (5.20b) are not actual dynamical perturbations but rather a result of our choice for the origin of the coordinate system.

Similarly, the solution for region 2 is,

$$\left.\begin{aligned}
u_2{}^* &= \tilde{y}/2 + 0.366\tilde{y}\epsilon^2 + 0(\epsilon^3) \\
v_2{}^* &= 0 \\
h_1{}^* &= \left[1 - (\tilde{y})^2/8\right] - 0.183(\tilde{y})^2\epsilon^2 + 0(\epsilon^3)
\end{aligned}\right\} \tag{5.20c}$$

which in the (x*,y*) coordinates can be written as,

$$u_2^* = (y^* + 4\sqrt{2})/2 - \sqrt{2}\cdot\varepsilon + 0.366(y^* + 4\sqrt{2})\varepsilon^2 + 0(\varepsilon^3)$$

$$h_2^* = \left[1 - \left(y^* + 4\sqrt{2}\right)^2/8\ \right] + \varepsilon\left(y^* + 4\sqrt{2}\right)\sqrt{2}/2$$

$$- \left[0.183\left(y^* + 4\sqrt{2}\right)^2 + 1\right]\ \varepsilon^2 + 0(\varepsilon^3)$$

$$v_2^* = 0$$

$$(5.20d)$$

For region 3, the solution is,

$$u_3^* = -y^*/2 + 1.861\varepsilon + 0(\varepsilon^2)$$

$$h_3^* = 1 - (y^*)^2/8 + 2.632\varepsilon + 0(\varepsilon^2)$$

$$\gamma_3^* = 1.316\varepsilon + 0(\varepsilon^2)$$

$$v_3^* = 0$$

$$(5.21)$$

Note that since γ_3^*, the width of the intrusion around the cylinder, is
not zero for $\varepsilon \neq 0$ there <u>must</u> always be a flow around the cylinder as
stated before. Recall that the solution in regions 1 and 2 had to be
carried to $0(\varepsilon^2)$ because otherwise the continuity and torque constraints
would not have been sufficient to close the problem. The flow in region 2
remains unaltered to $0(\varepsilon)$; the portion of the eddy flux that is "blocked"
by the cylinder is simply diverted from its original position to the
perimeter of the solid cylinder. The solution demonstrates that, no matter
how small the penetration of the cylinder into the vortex, a current
engulfing the cylinder must always be present.

g)   <u>Impossibility of rotational motion around the solid cylinder</u>: It is
known from the theory of point vortices in potential flow that, when a
point vortex is placed near a solid wall, a translatory motion of the whole
vortex is established. One can, therefore, ask whether or not the padlock
flow can rotate around the solid cylinder. Even though we have not stated
it specifically, we have effectively assumed in our foregoing analysis that

-33-

such a situation is impossible. Namely, we have considered only flows
which are stationary.

It is a simple matter to show mathematically that a rotational motion
of the whole padlock flow cannot be established because of the impossibili-
ty of balancing the centrifugal force; this will be demonstrated in the
following analysis. Before doing so, however, it is useful to consider the
cause of the migratory motion in the linear homogenous case (i.e., a
barotropic point vortex situated near a wall). The cause can easily be
traced to the fact that the mass flux is initially not balanced. Specifi-
cally, suppose that, at $t = 0$, a vortex is suddenly cut by an infinitely
long plate which represents a wall; at $t > 0$ the plate is situated at, say,
distance w from the eddy center. Under such conditions, the initial mass
flux between the vortex center and the wall is smaller than the vortex flux
away from the wall. Since vorticity is conserved, the distance between the
eddy center and the wall cannot accommodate the larger undisturbed eddy
flux.

As a result, the whole vortex starts migrating along the wall. The
drift adds to the absolute speed (and, hence, to the mass flux) in the
region between the center and the wall and subtracts from the speed in the
area between the center and the region away from the wall. This is done in
such a way that, when the eddy is migrating, the mass flux between the
center and the wall is equal to the flux between the center and the region
away from the wall. Consequently, there is no longer mass imbalance. In
our case (i.e., the padlock flow with vanishing depth along the edge) a
similar cause for a migration does not exist, i.e., because of the intru-
sions there is no imbalance in the mass flux. In view of this, it is
expected that there will not be any rotational migration in our case.

We shall now show, in a more quantitative fashion, that there is indeed no rotational motion. To show this, suppose, temporarily, that there is a steady rotational translation so that the whole padlock flow (shown in Fig. 6b) rotates counterclockwise around the center of the solid cylinder at an angular speed ω. Under such conditions, the flow in a coordinate system rotating at a rate ω appears to be steady and the governing momentum equations are (see e.g., Holton, 1972),

$$u \frac{\partial u}{\partial x} + v \frac{\partial u}{\partial y} - (f + 2\omega)v - \omega^2 x = -g' \frac{\partial h}{\partial x} \qquad (5.22a)$$

$$u \frac{\partial v}{\partial x} + v \frac{\partial v}{\partial y} + (f + 2\omega)u - \omega^2 y = -g' \frac{\partial h}{\partial y} \qquad , \qquad (5.22b)$$

where u and v are the speeds in the <u>rotating</u> system. In these equations, there are two new terms; the first ($2\omega v$ and $2\omega u$) is associated with a modification to the Coriolis parameter and the second ($\omega^2 x$ and $\omega^2 y$) is related to the centrifugal force.

By integrating (5.22b) over the whole volume of the padlock flow, taking into account the fact that the area is not a simply connected region and the known properties of line and surface integrals, one ultimately finds,

$$\frac{g'}{2} \oint h^2 dx = \omega^2 \iint_{-\infty}^{+\infty} hy\,dx\,dy \qquad , \qquad (5.23)$$

where the term on the left hand side is a <u>clockwise</u> integration around the solid cylinder.

The term on the right hand side of (5.23) represents the centrifugal force which is, of course, directed away from the center of the solid

cylinder [i.e., in the negative y direction (Fig. 6b)]. The term on the left, on the other hand, represents the pressure exerted by the cylinder on the padlock flow. Intuitively, one would expect the fluid pressure to be high in the region near the eddy (i.e, in the vicinity of point B in Fig. 6b) and low in the region away from the eddy (i.e., near point D). Consequently, the total integrated pressure on the cylinder will be directed at the positive y direction; the associated integrated pressure on the padlock flow will be directed in the opposite sense (i.e., the negative y direction). The two terms in (5.23) are, therefore, directed in the same sense (i.e., the negative y direction) and cannot balance each other. Hence, we conclude that there is no force to balance the centrifugal force induced by the migratory motion and, consequently, there will not be any rotation around the cylinder.

h)   Relationship between the final flow and the initial state: The detailed structure of the initial state depends, of course, on the way that the padlock flow is established (see Section 3a). Suppose, for a moment, that the padlock flow was formed by forcing the solid cylinder into a vortex. Since the padlock flow has zero potential vorticity and we saw earlier that potential vorticity is altered during the transient intrusion process, the vortex which was originally present prior to the forcing of the cylinder had potential vorticity different from zero. As mentioned, the value of this "initial" potential vorticity is not important for our analysis because we did not intend to solve the time-dependent problem. We assumed, however, that there exists an initial state which leads to a zero potential vorticity padlock flow. By considering the fact that the total volume of the fluid is conserved during the transient adjustment process,

one finds that, a) the central depth of the original vortex must have been $\sim O(\varepsilon^2 \hat{h})$ higher than the maximum final depth $(\hat{h})$, and b) the original radius was $O(\varepsilon^2 R_d)$ larger than the final radius in region 1.

6. General comments

Before discussing the application of our results to actual merging in the ocean, it is appropriate to comment on the "replacement" of one of the interacting eddies by a solid cylinder. An obvious similarity between a colliding eddy and a colliding cylinder is that both features are expected to exert a pressure on the eddy as they collide with it, and both features have similar geometry in the x, y plane. As we saw earlier, the exerted pressure is the key to the merging process and, therefore, it is believed that a solid cylinder provides an adequate "analog."

However, there are also some important differences between the solid cylinder and an actual eddy. For example, although both the actual eddy and the solid cylinder are subject to pressure forces, the former can adjust itself to the surrounding pressure, whereas the latter remains unaltered. In addition, as pointed out earlier, the actual eddy is drained via the intrusions so that a steady state is not reached before a complete merging is achieved.

While we should be on guard against oversimplified models (such as this one may seem, at first, to be), attacking the complete merging problem analytically appears to be hopeless. Even numerical integrations cannot provide the desired solution because of the difficulty in handling fronts $(h = 0)$. Some simplifications are, therefore, necessary and examination of

the cylinder-eddy interaction is useful for understanding the basic processes in question. Namely, the results of our analytical study pinpoint the effects which one should look for in more complicated and more realistic models. For example, laboratory experiments appear to be a natural tool for examining the complete problem. The results of such a study support the present findings and are reported in Nof and Simon (1986).

As far as the application of our general merging process to Cresswell's (1982) study is concerned, it appears that the essential dynamics may be similar. Because of the simplifications involved, a detailed quantitative comparison is, obviously, impossible. However, the fact that our model suggests a mechanism for eddy merging is, of course, in agreement with Cresswell's observations. The time scale for merging [relation (2.2) which gives $\sim$ 30 days for $\varepsilon = 0.1$ and $f \sim 10^{-4}$ sec^{-1}] is also appropriate even though it is difficult to say what the actual value of ε should be.

A potentially serious difference between Cresswell's observations and the present study is the fact that Cresswell's eddies were with unequal densities whereas our model addresses eddies with identical densities. It is easy to see, however, that such a difference is not major because all that it implies is that the mean position of the intrusions along the rims will not be taking place on the same level. Instead, the mean position of the intrusions will take place on different levels as shown schematically in Fig. 9. The major cause of the merging — the establishment of a mutual boundary with a nonzero vanishing depth — is present in both the collision of eddies with equal densities and the collision of eddies with unequal densities. The laboratory experiments of Nof and Simon (1986) on eddies with unequal density support these considerations.

An additional aspect of Cresswell's study that is not present in our study is the observation of a clockwise migration of the entire eddies (Fig. 1). It is difficult to say what the causes of such an effect could be but it might be a result of the transient merging process which we have not studied in detail.

7. Summary

A conceptual model for the merging of two isolated lens-like eddies has been developed with the assumptions that: i) the eddies are embedded in an infinitely deep barotropic fluid; ii) with the exception of shock waves which are presumed to be present during the transient merging process, all motions are frictionless and hydrostatic.

Our attention has been focused on two lens-like eddies (with equal densities) which are pushed against each other by a mean flow that relaxes after the eddies are in contact. It is argued that the establishment of a "figure eight" structure (associated with a mutual boundary with a nonzero depth) forces the generation of "tentacles" and "arms." These features correspond to intrusions along the eddies' edges; they result from the fact that particles along the peripheries do not have sufficient energy to rise to the mutual nonzero depth (Fig. 2). The establishment of tentacles causes the eddies to wrap around each other (Fig. 3). As time goes on, the tentacles become longer and longer so that they effectively "drain" the vortices. Ultimately, a single vortex corresponding to two adjacent spirals is formed (Fig. 4).

While the details of the above process can be easily described in a qualitative manner, it is impossible to prove the complete process

analytically because it is both nonlinear and three-dimensional (x, y, t). It is, however, possible to prove analytically that the establishment of tentacles is inevitable. To show this, we have conceptually replaced one of the interacting vortices by a solid cylinder (Figs. 5 and 6). This simplification removes the time dependency from the problem because there is now only one tentacle which, upon engulfing the cylinder, forms a steady "padlock" flow. Using a constraint associated with the conservation of torque (i.e., moment of momentum) and a perturbation scheme, we have constructed the detailed solution even though the simplified problem is nonlinear.

With the aid of the above model, it has been shown that two lens-like eddies which are compressed against each other will merge within the period $\sim O(\epsilon^{5/2} f)^{-1}$ [where ϵ is the relative distance that each vortex is squeezed]. It is argued that during the merging the potential vorticity of the vortices is altered via the action of shock waves near the nose of the tentacles. This is based on: a) several studies [e.g., Griffiths (1986)] which have shown that transient intrusions contain breaking waves or shocks and b) a recent study (Nof, 1986b) which illustrated that shock waves cause major alterations in the potential vorticity. The details of the potential vorticity alteration by the action of shock waves in the intrusion is quite complicated and is beyond the scope of this study; it will be the focus of a future investigation.

Because of the difficulties involved in analytically (or numerically) analyzing the complete merging process, laboratory experiments are a natural extension of the present investigation. One such study is the laboratory experiment of Nof and Simon (1986) where the coalescence process has been examined in detail. For a comprehensive description the reader is

referred to the above article but it is worth pointing out here that the laboratory experiments support the contention that merging takes place via the establishment of tentacles, and that potential vorticity is indeed altered during the merging.

8. Acknowledgements

APPENDIX

List of Symbols

A_1, B_1 Integration constants associated with (5.1)

A_3, B_3 Integration constants associated with (5.7) and (5.8). Their relationship to $\gamma_3^{(1)}$ is given by (5.12).

b Radius of eddy for energy calculations (Section 1).

E Total energy (kinetic plus potential).

f The Coriolis parameter.

g' "Reduced gravity" ($g\Delta\rho/\rho$ where g is the gravitational acceleration and $\Delta\rho$ is the density difference between the layers).

$\hat{h}$ Maximum depth of vortex (i.e., depth at the point of no speed); it is also the maximum depth of the padlock flow at point A.

h_B Depth at point B (Fig. 2).

h^* Nondimensional depth ($h/\hat{h}$).

i, f Section 2 — subscripts which denote the initial and final state (respectively). In Section 3, "i" (1, 2, 3) denotes association with various regions (3.1).

Q Volume of vortex.

r Radius in polar coordinates whose origin is located at the center of the solid cylinder.

R_d Deformation radius $(g'\hbar)^{\frac{1}{2}}/f$.

r_0 In Section 3 — radius of solid cylinder (Fig. 6b); in Section 4 it is shown that, for our case, r_0 is also the radius of the undisturbed vortex, $2(2g'\hbar)^{\frac{1}{2}}$.

$r*$ Nondimensional radius in a polar coordinates system with an origin at the center of the cylinder.

$\tilde{r}, \tilde{\theta}$ Nondimensional radius and angle in a polar coordinate system whose origin is located at the center of the undisturbed vortex (i.e., center of padlock flow).

t_m Merging time.

u_A, u_B Speed along the x axis (i.e., in a Cartesian coordinates) for points A and B (Fig. 2).

u, v Speeds in Cartesian coordinates whose origin is located at the center of the solid cylinder (Fig. 6b).

$u*$, $v*$ Nondimensional speeds in Cartesian coordinates whose origin is located at the center of the solid cylinder (Fig. 6b).

$u^{(0)}$, $v^{(0)}$, $h^{(0)}$ Velocity and depth (in Cartesian coordinates located at the of the solid cylinder) of the undisturbed vortex.

$\tilde{u}^{(0)}$, $\tilde{v}^{(0)}$, $\tilde{h}^{(0)}$ The undisturbed velocity and depth in a Cartesian coordinate system located at the center of the undisturbed vortex.

$u^{(1)}$, $v^{(1)}$, $h^{(1)}$, $u^{(2)}$, $v^{(2)}$, $h^{(2)}$ First and second-order perturbations to the basic flow (in Cartesian coordinates located at the center of the solid cylinder).

$v_{\theta i}$ Initial orbital speed in polar coordinates whose origin is situated at the center of the vortex.

$\tilde{v}_{\theta}$, $\tilde{h}$ Nondimensional orbital speed and depth in a polar coordinates whose origin is located at the center of the undisturbed vortex.

w   The distance between the center of a point vortex and a wall (Section 5).

x, y, t   Space and time coordinates in a Cartesian coordinates whose origin is situated at the center of the solid cylinder.

$\tilde{x}$, $\tilde{y}$ Space in a Cartesian coordinates located at the center of the undisturbed vortex (point A, Fig. 6b). It is related to x, y by, $y = \tilde{y} 2\sqrt{2}\, (2 - \epsilon)$; $x = \tilde{x}$.

x^*, y^* Nondimensional Cartesian coordinates in a system whose origin is situated at the center of the solid cylinder.

α An integration constant associated with the solution of (4.1).

γ_1 Distance between the edge of the padlock flow (in region 1) and the edge of the undisturbed vortex (nondimensionalized by $2\sqrt{2}R_d$).

γ_3 Distance between the edge of the intrusion (in region 3) and the surface of the solid cylinder (nondimensionalized by $2\sqrt{2}R_d$).

δ A nondimensional coefficient associated with the second-order flow in region 2. It is found to be equal to 0.366.

ε   In Section 2 — the distance that each vortex is "pushed" into the other (Fig. 2); in Section 3 — the distance between the edge of the undisturbed vortex and the edge of the cylinder (Fig. 6b). Note that the undisturbed vortex is defined as a zero potential vorticity lens which is aligned with the center and depth of the padlock flow (i.e., it has the same center and depth as the padlock flow).

ψ Stream function.

ψ^* Nondimensional stream function.

ω The rate at which the padlock flow rotates around the solid cylinder. In Section 5 it is shown that it is zero.

$\oint, \oint$ Integration in a counterclockwise (clockwise) manner along a closed curve.

REFERENCES

Benjamin, T. B. (1968): Gravity currents and related phenomena. J. Fluid Mech., 31: 209-248.

Cheney, R. E. (1977): Synoptic observations of the oceanic frontal system east of Japan. J. Geophys. Res., 82: 5459-5468.

Christiansen, J. P. and N. J. Zabusky (1973): Instability, coalescence, and fission of finite-area vortex structures. J. Fluid Mech., 61: 219-243.

Cresswell, G. R. (1982): The coalescence of two East Australian Current warm-core eddies. Science, 215: 161-164.

Cresswell, G. R. and R. legeckis (1986): Eddies off southeastern Australia, 1980/81. To appear in Deep-Sea Res.

Gill, A. E. (1982): Atmosphere Ocean Dynamics. Academic Press, 662 pp.

Gill, A. E. and R. W. Griffiths (1981): Why should two anticyclonic eddies merge? Ocean Modelling, 41: 10-16.

Griffiths, R. W. (1986): Gravity currents in rotating systems. Ann. Rev. Fluid Mech., 18: 59-89.

Griffiths, R. W. and E. J. Hopfinger (1983): Gravity currents moving along a lateral boundary in a rotating fluid. J. Fluid Mech., 134: 357-399.

_____ and _____ (1986a): Experiments with baroclinic vortex pairs in a rotating fluid. J. Fluid Mech., in press.

_____ and _____ (1986b): Coalescing of geostrophic vortices. Submitted to J. Fluid Mech.

Holton, J. R. (1972): An Introduction to Dynamic Meteorology. Academic Press, New York, 319 pp.

Kubokawa, A. and K. Hanawa (1984): A theory of semigeostrophic gravity waves and its application to the intrusion of a density current along a coast. Parts I and II. J. Oceanogr. Soc. Japan, 40: 247-270.

Lai, D. Y. and P. L. Richardson (1977): Distribution and movement of Gulf Stream rings. J. Phys. Oceanogr., 7: 670-683.

McWilliams, J. C. (1983): Interactions of isolated vortices. II. Modon generation by monopole collision. Geophys. and Astrophys. Fluid Dyn., 24: 1-22.

McWilliams, J. C. and N. J. Zabusky (1982): Interactions of isolated vortices. I. Modons colliding with modons. Geophys and Astrophys. Fluid Dyn., 19: 207-227.

Melander, M. V. , N. J. Zabusky and J. C. McWilliams (1985): A model for symmetrix vortex-merger. Presented at Third Army Conf. on Appl. Math. and Computing. To be published in proceedings of the meeting.

Mied, R. P. and G. J. Lindemann (1984): Mass transfer between Gulf Stream Rings. J. Geophys. Res., 89: 6365-6372.

Nof, D. (1981a): On the dynamics of equatorial outflows with application to the Amazon's basin. J. Mar. Res., 39: 1-29.

_____ (1981b): On the β-induced movement of isolated baroclinic eddies. J. Phys. Oceanogr. 11: 1662-1672.

_____ (1986a): The collision between the Gulf Stream and warm-core rings. Deep-Sea Res., 33: 359-378.

_____ (1986b): Geostrophic shock waves. J. Phys. Oceanogr., 16: 886-901.

_____ (1986c): Penetrating outflows and the dam-breaking problem. Submitted to J. Mar. Res.

Nof, D. and L. Simon (1986): Laboratory experiments on the merging of anticyclonic eddies. Submitted to J. Phys. Oceanogr.

Overman, E. A. and N. J. Zabusky (1982): Evolution and merger of isolated vortex structures. Phys. Fluids, 23: 2339-2342.

Ring Group (1981): Gulf Stream cold-core rings: Their physics, chemistry, and biology. Science, 212: 1091-1100.

Simpson, J. E. (1982): Gravity currents in the laboratory, atosphere, and ocean. Ann. Rev. Fluid Mech., 14: 213-234.

Stern, M. E., J. A. Whitehead and B. L. Hua (1982): The intrusion of a density current along the coast of a rotating fluid. J. Fluid Mech., 123: 237-265.

Young, W. R. (1985): Some interaction between small numbers of baroclinic geostrophic vortices. Geophys. Astrophys. Fluid Dyn., 33: 35-61.
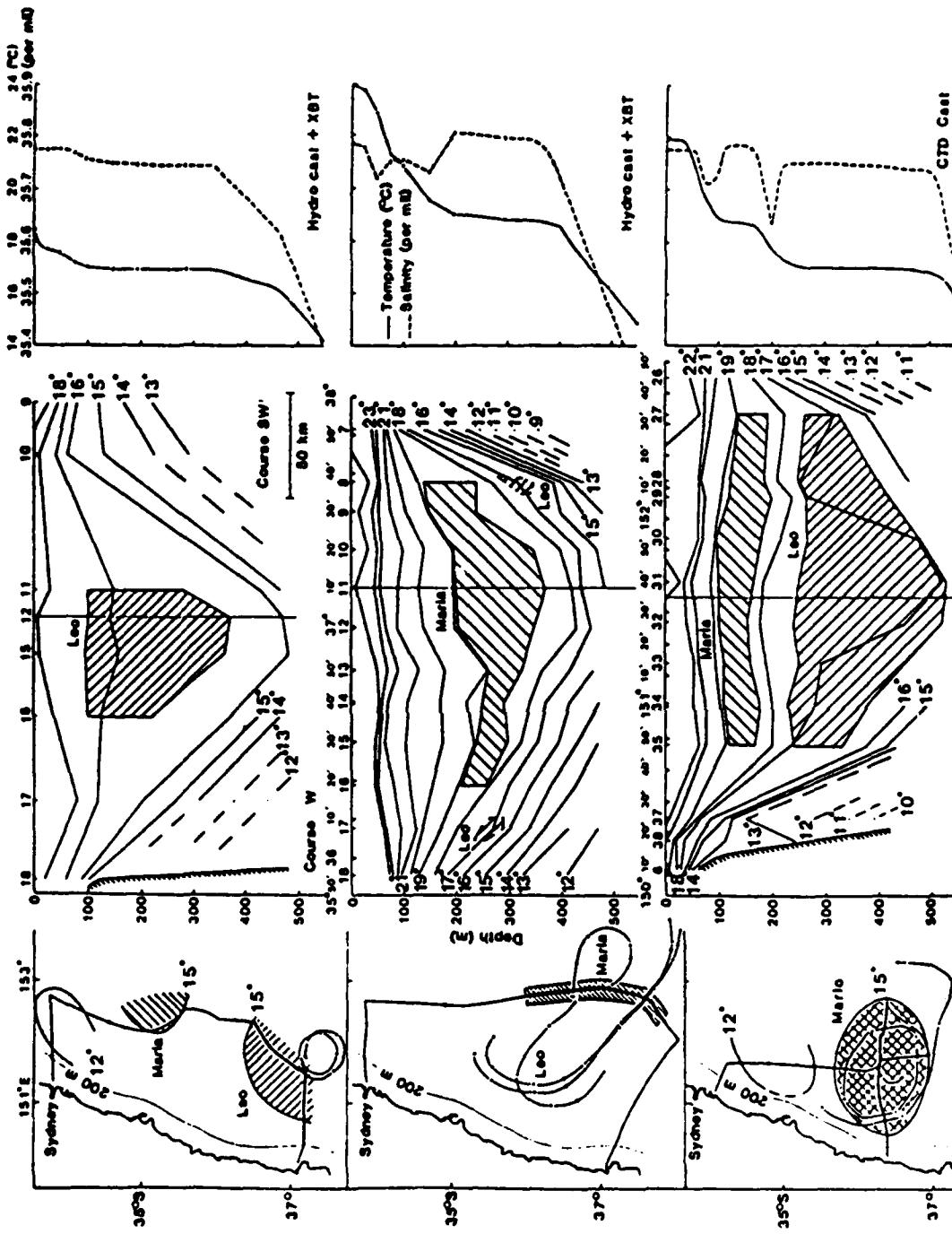
Figure 1. The merging of two anticyclonic eddies off East Australia (adopted from Cresswell 1981). The results of Cresswell's ship surveys for December 1980, January 1981 and April 1981 are shown on top, middle, and bottom (respectively). In column 1 buoy tracks for several days before and after the surveys are marked; regions having 250-m temperatures exceeding 15°C are shaded; the 12°C isotherm for 250 m is marked. The thickened ship tracks define the temperature sections (in degrees Celsius) in column 2 where the signature layers of eddies Leo and Maria are shaded. The vertical lines in column 2 indicate the positions for the temperature and salinity profiles of column 3.
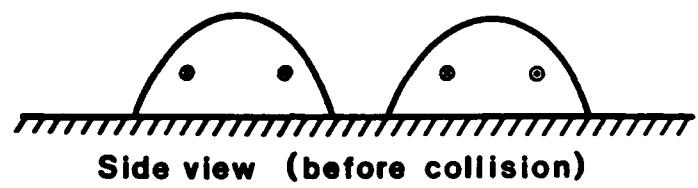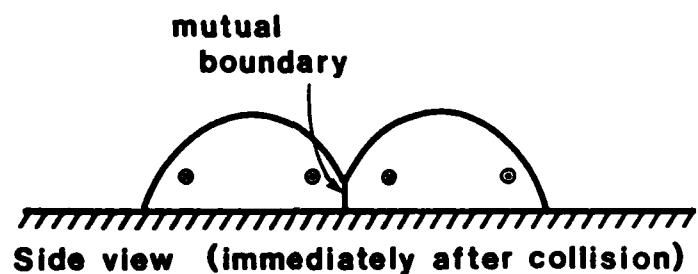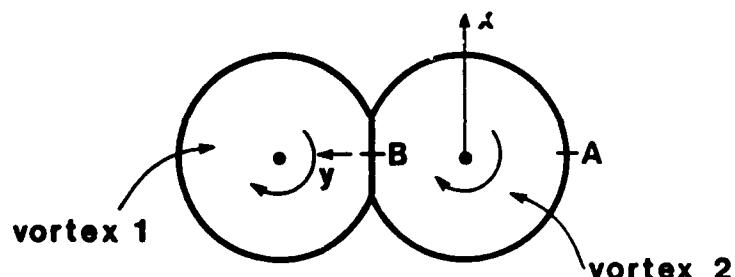
Figure 2.   Schematic diagram of the interaction of two isolated
            lens-like eddies. A side view of the eddies prior to any
            contact is shown on top. The middle and lower panels
            display the side and top views of two eddies which are
            touching each other due to, say, an advective current.
            The shape shown in the lower panel is referred to as the
   "figure eight" structure.

intrusion of vortex 1
along the edge of
vortex 2

intrusion of vortex 2 along
the edge of vortex 1
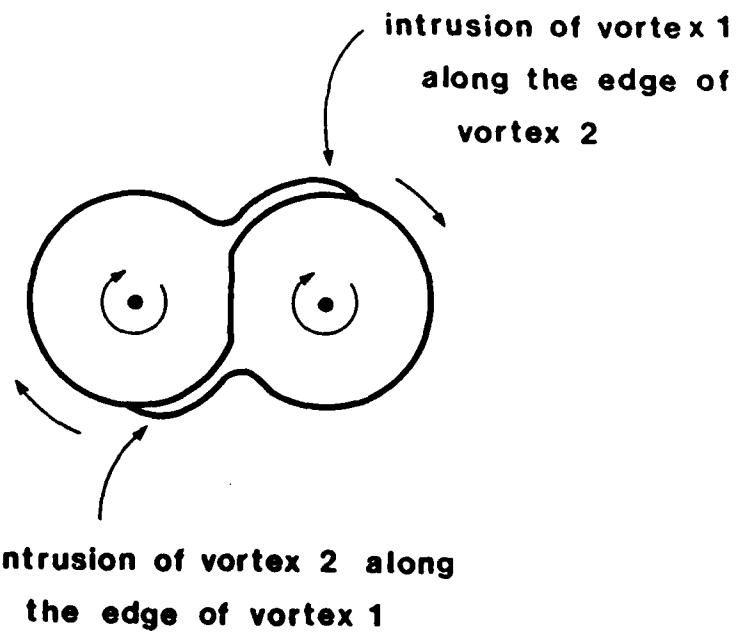
Figure 3.   The beginning of the double intrusion along the edges of
the eddies.
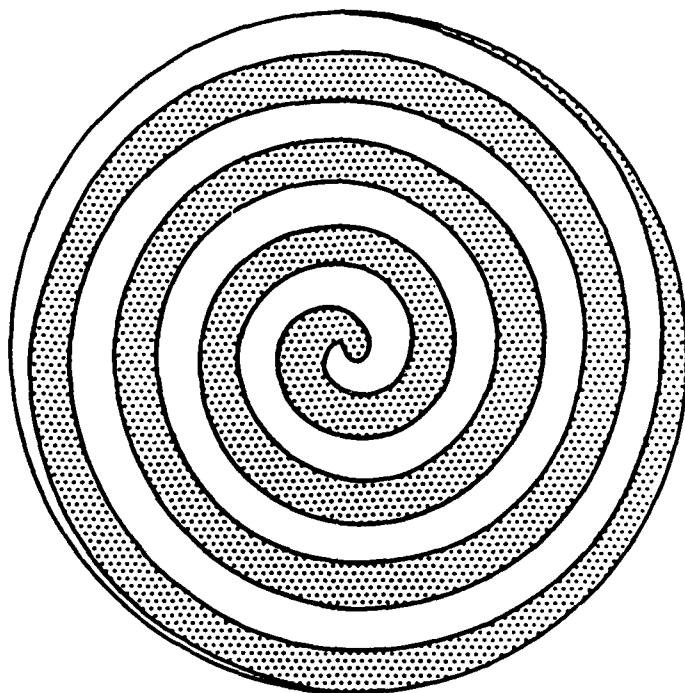
Figure 4b. Schematic diagram of the edge intrusion in the final
            stage.   Note that complete merging occurs because the
   intrusions "leak" all the fluids of the vortices.
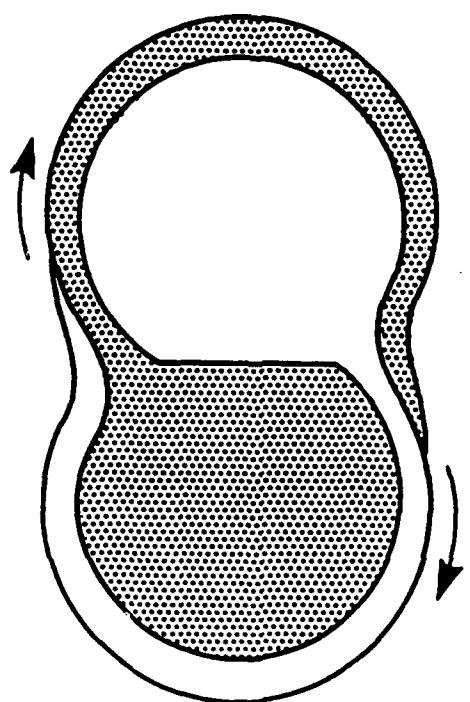
Figure 4a.   Schematic diagram of the edge intrusion in an advanced
   stage.
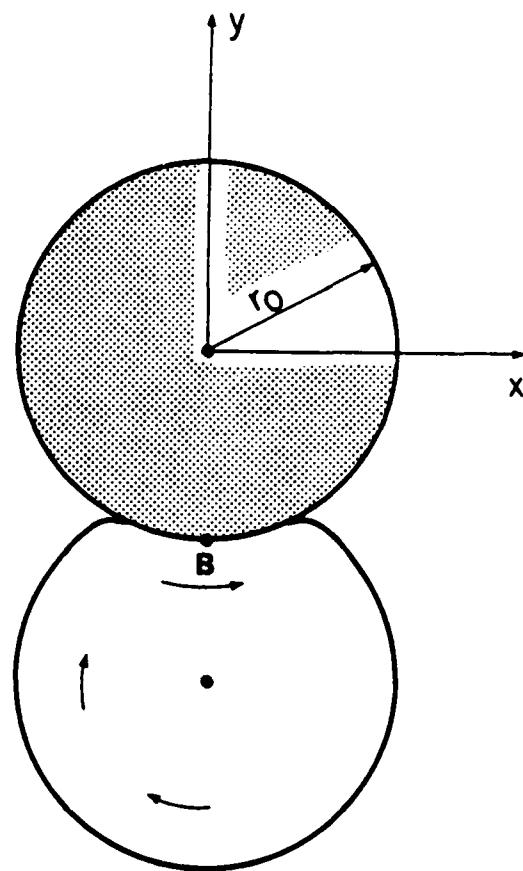
Figure 5.   A schematic diagram of a hypothetical response to a
forced cylinder.   The vortex is adjacent to the solid
cylinder which has been slightly forced into it.   The
diagram illustrates an adjustment which is confined to
the contact area; as shown in the text such a situation
cannot exist.   Instead, there must be an intrusion around
the cylinder (Fig. 6a) so that, ultimately, a "padlock"
flow is established (Fig. 6b).
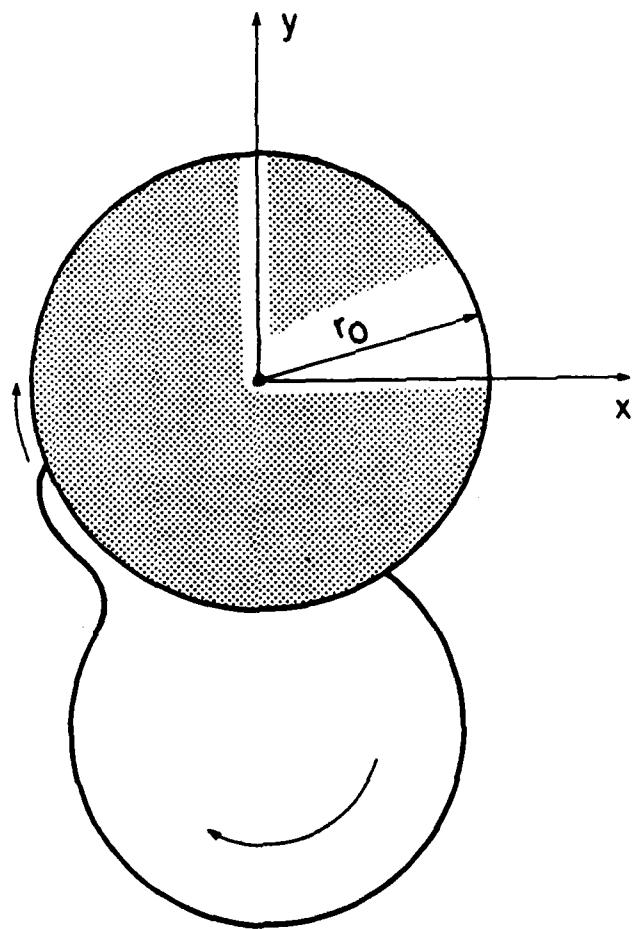
Figure 6a. The initial intrusion stage. Ultimately, the intrusion reattaches itself to the eddy and a steady "padlock" flow is established.
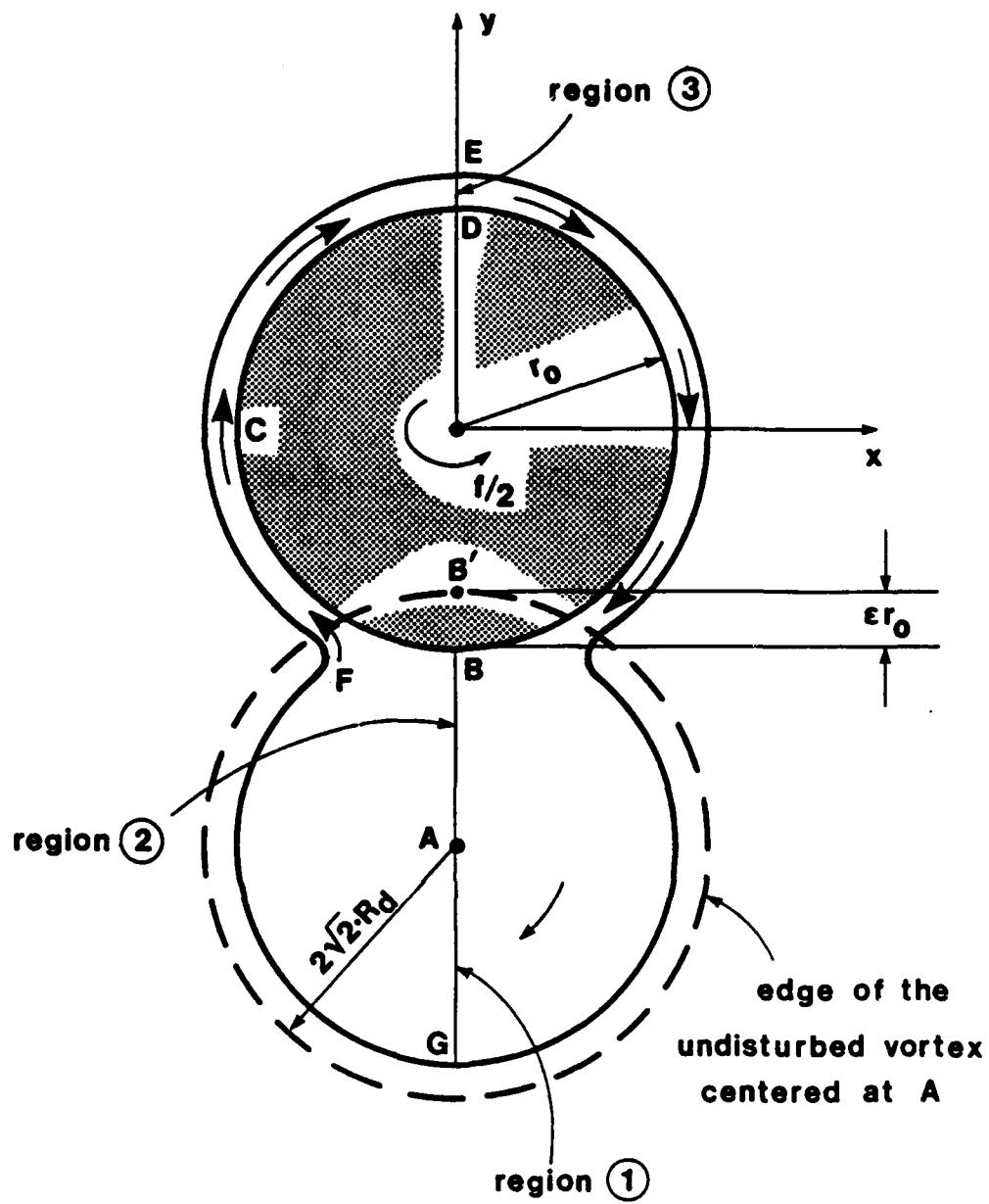
Figure 6b. Schematic diagram of the "padlock" flow. Point A is defined as the point at which the speed of the padlock flow vanishes; $\hat{h}$ is the depth at A and the radius of the undisturbed vortex (which is centered at A and has a maximum depth $\hat{h}$) is $2\sqrt{2}R_d$ [where $R_d = (g'\hat{h})^{\frac{1}{2}}/f$].
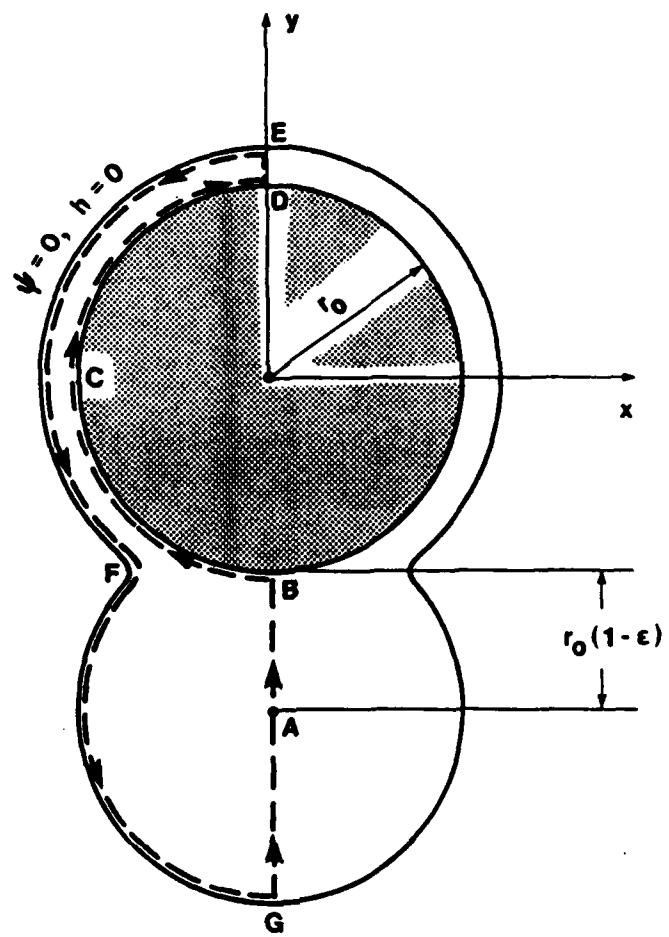
Figure 7. An illustration of the integration area for the computation of the torque associated with the padlock flow.
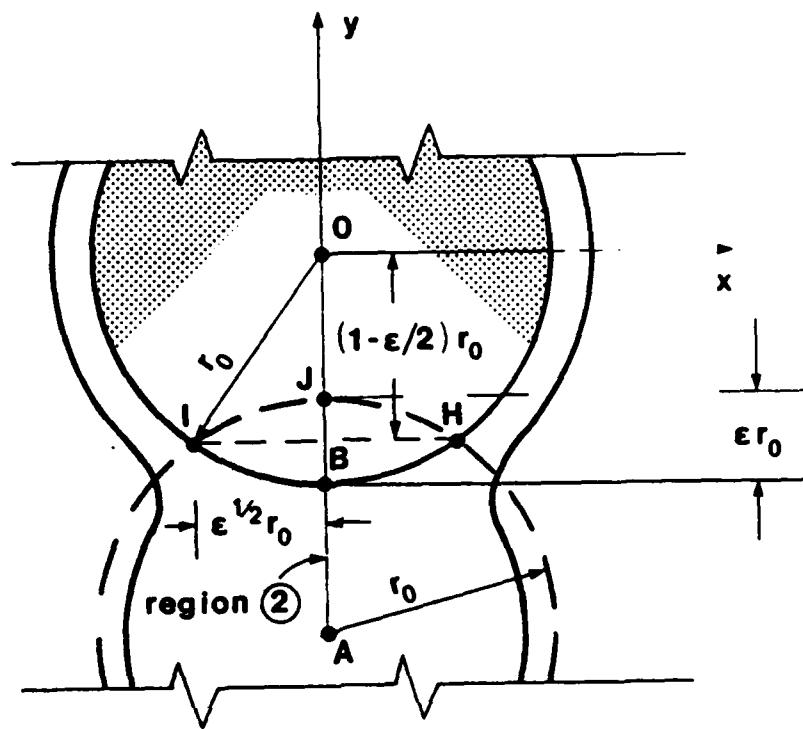
Figure 8.   The geometry in the vicinity of region 2.

intrusion of
vortex 2

intrusion of
vortex 1

① ②

Eddies with equal densities

intrusion of
vortex 2

intrusion of
vortex 1

heavy ① ② light
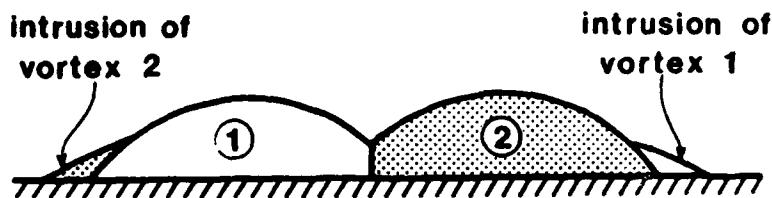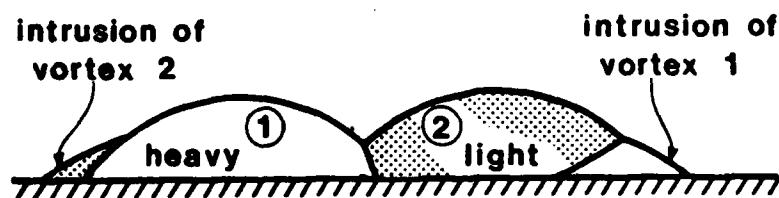
Eddies with unequal densities

Figure 9.   A cross-section of pairing vortices. The upper panel
            shows eddies with identical densities; their merging is
            qualitatively displayed in Figs. 3 and 4. The lower
            panel displays eddies with unequal densities. While the
            merging is generated by the establishment of a mutual
            boundary with a nonvanishing depth as in the equal
            density case, the final situation is different from that
            displayed by Fig. 4c. Here, instead of forming two
            adjacent spirals, the lighter vortex is "climbing" on top
            of the heavier lens. This is supported by the laboratory
            experiments of Nof and Simon (1986).

END

7-81

DTIC